



Assessment of liquefaction of silty soils using combined experimental and theoretical results

Betegard Jeudy¹, Mourad B. Karray² Chekired Mohamed³

¹ Ph.D. Student, Department of Civil and Building Engineering, University of Sherbrooke - Sherbrooke, QC, Canada.

² Professor, Department of Civil and Building Engineering, University of Sherbrooke - Sherbrooke, QC, Canada.

³ Senior Engineer, Hydro-Québec, Montréal, Québec, Canada

ABSTRACT

Field tests (e.g. SPT, CPT) based methods had been largely used to assess the liquefaction potential of granular materials, but they can underestimate the liquefaction resistance of fine-grained soils. Although susceptibility criteria have been developed for fine-grained soils, they are considered unreliable because some external factors like the cyclic loading and the stress history were not considered. In this paper, a new approach based on experimental and theoretical results is used to assess liquefaction potential of silts by considering the effects of the generated pore pressure and the soil degradation on the cyclic resistance. The experimental results include measurements of shear wave velocity, V_s in laboratory and a series of cyclic combined triaxial simple shear (TxSS) tests to assess their dynamic characteristics. Theoretical results consist of theoretical behavior models calibrated on the experimental test results and relationships between the pore pressure, the dissipated energy and the soil degradation to perform numerical simulations of the dynamic characteristics using FLAC software. The comparison between the computed cyclic resistance and those obtained from direct shear tests (DSS) and from previous studies on other silts shows that this new approach can be used as an alternative to existing liquefaction assessment methods.

Keywords: Liquefaction, shear wave velocity, silt, cyclic resistance, energy concept.

INTRODUCTION

Earthquakes are amongst the most devastating natural events in the world. During the past years, most of them had caused a lot of damages and loss of life. During these events, some damages are in the most cases induced by ground amplification and by soil liquefaction. About liquefaction, it is particularly associated with the behavior of loose saturated sandy soils. As results, significant database exists on liquefaction of sandy soils. The simplified procedure of liquefaction triggering using standard penetration test blow count, $N-SPT$ [1] had been widely used. Others in situ measurements (e.g., cone penetration resistance, q_c -CPT; and shear wave velocity, V_s) had been more and more used in liquefaction evaluation ([2], [3]). The in-situ soil resistance, represented by the cyclic resistance ratio, CRR are evaluated from correlations with the normalized standard penetration resistance, $(N_1)_{60}$, the normalized static cone penetration resistance, q_{c1N} , and the normalized shear wave velocity, V_{s1} . Laboratory monotonic and cyclic tests can be performed to evaluate directly the cyclic resistance of the soil or indirectly from correlations and from numerical simulations. The induced seismic stress in a soil layer is represented by the cyclic stress ratio (CSR), defined as the amplitude of the cyclic shear stress (τ_c) divided by the initial effective confining pressure (σ'_{v0}). Although τ_c is variable in the field because of the nature of the ground accelerations, it is replaced by constant cyclic stress in laboratory. Then, the cyclic stress ratio in a soil layer can be estimated by the eq. (1):

$$CSR = \frac{\tau_c}{\sigma'_{v0}} = 0.65 \frac{a_{max}}{g} \frac{\sigma'_{v0}}{\sigma'_{v0}} r_d \quad (1)$$

Where a_{max} is the peak horizontal ground acceleration; g is the acceleration of gravity; σ'_{v0} is the total vertical overburden; σ'_{v0} is the vertical effective overburden pressure acting at the same depth before the earthquake; r_d is the shear stress reduction coefficient which decreases with the depth [2]. The comparison between the cyclic stress ratio (CSR) induce by the earthquake and the cyclic resistance ratio (CRR) of the soil can be used to evaluate the potential of liquefaction of the soil and liquefaction charts. This approach was developed for sandy soils containing less than 35% fines. However, recent earthquakes have shown that the loss of strength and rigidity (cyclic softening) in fine-grained soils can induce severe damage comparable to those observed liquefaction of sandy soils ([4], [5]). The first stools generally used for assessment of liquefaction of fine-grained soil were the susceptibility criteria like the chines criteria or the Seed and Idris criteria which were mainly based on field observations during historic earthquakes [6]. However, these criteria are very limited and not considered some factors that have

real effects on the soil response such as stress history, amplitude and duration of cyclic loading ([5], [7]). Moreover, the use of these criteria would cause significant errors, because a soil can be classified liquefiable while it is not and vice versa. [8]. Thus, it is generally recommended to use laboratory tests to assess the liquefaction potential of fine-grained soils [4]. This study presents a new approach to assess the liquefaction or the cyclic softening of soils. The procedure combines both practice and theory to define the cycling shear resistance and cyclic behavior of soils.

PHYSICAL PROPERTIES OF THE TESTED SOIL SAMPLES

In this study, three silty soils are used. The first material is sandy silt extracted between 3.8 and 4.0 m depth from a deposit at the Laurentides station site in Charlesbourg borough, Québec. It consists mainly of a very dense till with presence of alluvium in the north of the station. In this area, the soil has a natural frequency of $f_0=4.27$ Hz. Thus, the frequency of 4.0 Hz comparable to the deposit is considered to test all samples. The intact sandy silt (30 % of sand), with graded particles size distribution, has a coefficient of uniformity, $c_u=49$ and a curvature coefficient $c_c=1.8$. Its plastic index is 9.8% and its liquidity limit is 24.6%. According to the USCS classification system, the soil is classified as CL. The second material is the same L-TM2 sandy silt in which the sand particles (> 0.16 mm) are removed. The last material was extracted from a site of the new Champlain bridge in Montreal city. This site consists generally of fill material (silty sand) with thicknesses varying from approximately 1 to 11 m and underlain by glacial till overlying shale rock. In some areas, a silty soil layer is encountered between the fill and the till. This silt layer varies in thickness from about 2 to 8 m and has a variable density ranging from very loose to very dense. The sandy silt samples were tested in intact conditions whilst the silt samples are reconstituted. The its grain-size distribution curve is shown in Fig. 1(a).

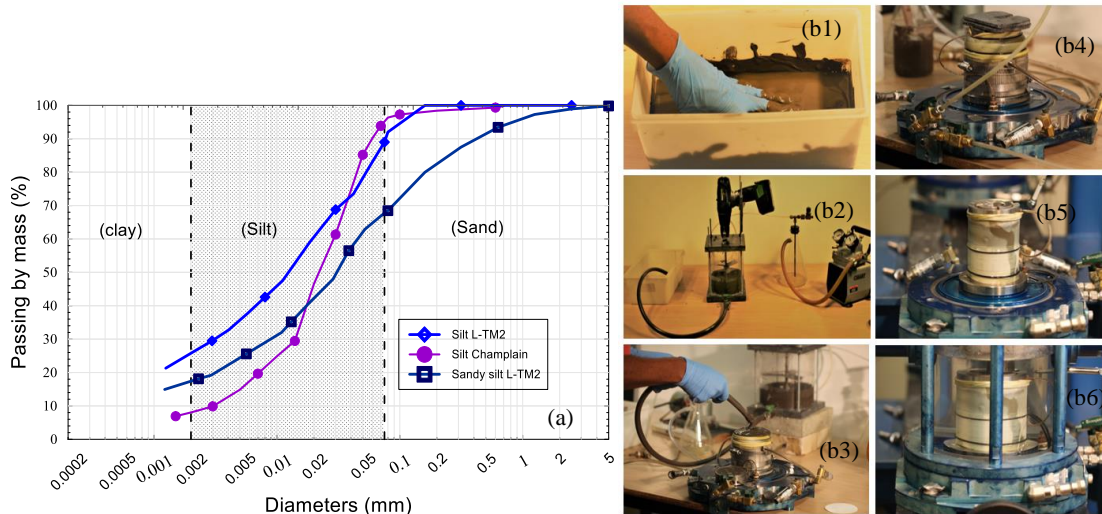


Figure 1. (a) Grain size distribution of the L-TM2 sandy silt, the L-TM2 silt and the Champlain silt (b)Preparation of reconstituted T_{vSS} silt samples.

SAMPLES PREPARATION

In the laboratory, soil behavior can be studied from intact and reconstituted specimens. Intact samples help to understand the actual soil characteristics in the field. However, for some soils, it is difficult to extract, to transport and to maintain intact samples. To study the behavior of these soils, reconstitution methods must be used. It is recommended that a deposition method should be suitable for the soil type and its natural deposition process. It should facilitate the reproduction of homogeneous samples with similar characteristics [9]. In this study, the slurry deposition method proposed by Poncelet [10] is used because it is a kind of water sedimentation technique adapted for the reconstitution of homogenous samples of fine-grained soils and in which we attempt to recreate the natural deposition process of silts. The preparation steps are shown in Fig. 1. Firstly, it consists of a manual homogenization of the dry soil and the amount of de-aired water required in a tank until we obtain a slurry with a water content well above the liquidity limit [Fig. 1(b1)]. The mixture is then drawn into a hermetic container provided with a rotary shaft which ensures the material mixing. A negative pressure of 40 to 70 kPa is applied for over 180 minutes to remove the trapped air bubbles in the mixture [Fig. 1(b2)]. The mixture is then transferred to the mold previously filled with water to simulate the deposition in the fluvial environment [Fig. 1(b3)]. The sample can be left standing for 90 to 180 minutes before removing the mold depending on the material. A small load of 1.0 to 2.5 kg and a suction of 4 to 10 kPa can be also applied to accelerate consolidation in the mold [Fig. 1(b4)]. Once the sample wrapped by a membrane becomes self-sustaining, demolding is done [Fig. 1(b5)]. Finally, it is placed in the cell which is then filled with water and pressurized according to the general

procedure of triaxial tests [Fig. 1(b6)]. After saturation, with a Skempton's B value greater than 0.94, the sample is isotopically consolidated. After consolidation, a cyclic loading under the undrained condition is applied to the sample until the occurrence of initial liquefaction or cyclic rupture.

LABORATORY TESTING AND RESULTS

Measurement of shear wave velocity (V_s) using P-RAT

The P-RAT has been developed in the geotechnical laboratory at Sherbrooke University [11]. The technique can be easily incorporated into conventional geotechnical apparatus such as triaxial and oedometer cells. In this study, it has been incorporated into an oedometer apparatus which allows shear wave velocity measurement during consolidation tests. The P-RAT system essentially consists of two parts: an emitter and a receiver (Fig. 2). Each part is a piezoelectric inert ring. The transceiver system is connected to a computer via acquisition and a wave generator card. The system comprises a signal generator connected to the piezoelectric transmitter ring. Between the generation of the signal and the transmitter, an amplifier of the signal power is used. The process consists of emitting a wave through the power amplifier to the piezoelectric transmitter ring which vibrates in the radial direction. Porous stone is fitted inside the ring using a special epoxy to allow the propagation of shear wave when the coupled ring-stone system is in contact with the soil specimen. The wave reaches the receiver ring that connected to an oscilloscope where its velocity is measured after signal processing.

The P-RAT has been used to determine the shear wave velocity of soils and to construct the relationship between the normalized shear wave velocity (V_{s1}) and the void ratio (e) of the tested soils. The value of V_{s1} can be estimated by the eq.(1) [12].

$$V_{s1} = V_s \left[\frac{P_a}{\sigma'_v} \right]^\beta \quad (1)$$

In this equation, P_a is normal atmospheric pressure in the same units as the effective vertical stress, σ'_v (i.e., $P_a \approx 100$ kPa if σ'_v is in kPa). The exponential β is taken to 0.25 for a variety of soil ranging from sand to clay ([13]; [14]).

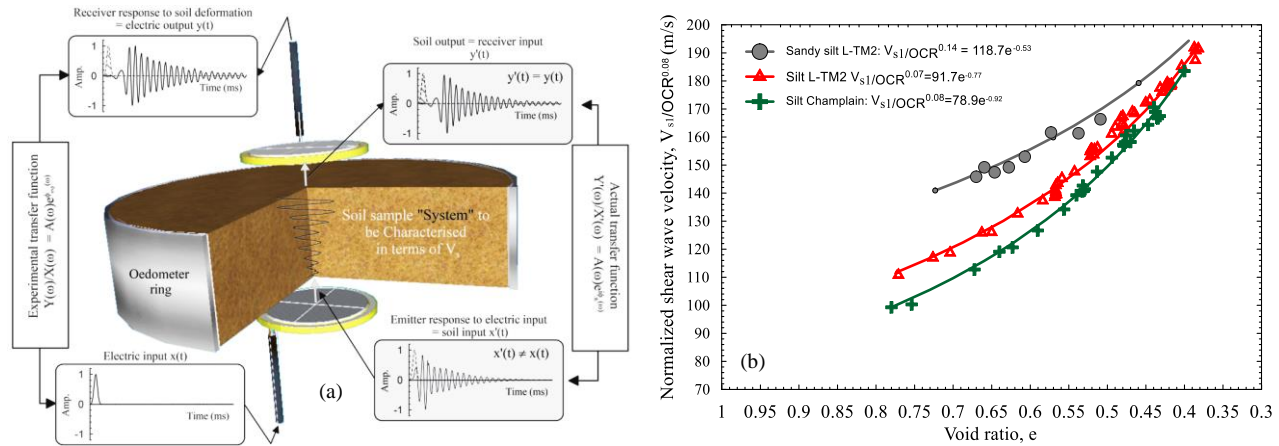


Figure 2. (a) Schematic of the experimental P-RAT test (Karray et al 2015); (b) Variation of the normalized shear wave velocity as a function of void ratio and OCR.

Typical normalized shear wave, V_{s1} curves are shown in Fig. 2(b) as a function of void ratio and OCR at power α which is equal to 0.14 for the L-TM2 sandy silt, 0.07 and 0.08 respectively for the L-TM2 silt and the Champlain silt. This figure shows the variation of V_{s1}/OCR^α with the void ratio, e . As expected, the sandy silt shows higher values of shear wave velocity than the other silts. For example, at OCR=1 and at a void ratio of 0.5, it has a V_{s1} of 172 m/s while the L-TM2 and Champlain silty samples show respectively 157 m/s and 150 m/s. The result may be due to the soil fabric effect and particles size distribution ([12], [15]). In this study, measurement of shear wave velocity, V_s in P-RAT tests are used to evaluate the small-strain shear modulus, G_{max} of the soils according to the relationship between V_s and the unit weight of the soil as shown in the eq. (2):

$$G_{max} = \rho V_s^2 \quad (2)$$

Cyclic T_xSS tests to evaluate the cyclic resistance ratio (CRR)

The cyclic shear tests are performed using the T_xSS apparatus which is a seismic simulator developed by the Institut de Recherche d'Hydro-Québec (IREQ) in collaboration with the Geotechnical laboratory at Sherbrooke University ([16]). This apparatus is designed to apply a simple shear test on samples in triaxial-test conditions. The device allows complete control of the cyclic shear strain which is the main factor to control the increase in the pore pressure and thus liquefaction. Thus, a series

of strain-controlled undrained T_xSS tests were performed according to the conditions summarized in tables 1 and 2. Typical T_xSS test results are shown in Fig. 3 for a reconstituted sample. The upper left plot Fig. 3(a) shows the increase of the pore pressure ($R_u = \Delta u/\sigma'_c$) as a function of the time in seconds which results in an exponential decay of the cyclic stress ratio (CSR) defined as the amplitude of the applied cyclic shear stress (τ_{cyc}) divided by the initial effective confining stress (σ'_c). Figure 3(b) shows the applied shear distortion curve and the increase in vertical axial deformation of the sample. Figure 3(c) shows CSR- γ_{cyc} hysteric loops rotate towards the γ axis with the increase in the time or in the number of cycles.

Table 1. T_xSS tests performed on the reconstituted L-TM2 silt and on the intact L-TM2 sandy silt.

Test No (silt)	γ_{cyc} (%)	σ'_c (kPa)	e_i	e_c	OCR	B	Test No (sandy silt)	γ_{cyc} (%)	σ'_c (kPa)	e_i	e_c	OCR	B
T_xSS-1	1.1	98	0.776	0.660	1	0.98	T_xSS-1i	0.60	53.0	0.697	0.665	6	0.92
T_xSS-2	0.65	98	0.77	0.636	1	0.95	T_xSS-2i	0.85	58.0	0.704	0.700	6	0.94
T_xSS-3	0.21	104	0.728	0.657	1	0.98	T_xSS-3i	1.04	59.0	0.722	0.708	6	0.95
T_xSS-4	0.92	104	0.710	0.591	2	0.95	T_xSS-4i	1.45	55.0	0.743	0.717	6	0.92
T_xSS-5	0.65	102	0.706	0.580	2	0.95	T_xSS-1i	0.60	53.0	0.697	0.665	6	0.92
T_xSS-6	1.90	104	0.736	0.557	2	0.95							
T_xSS-7	0.45	101	0.644	0.521	4	0.95							
T_xSS-8	0.95	103	0.747	0.540	4	0.97							
T_xSS-9	1.20	102	0.682	0.514	4	0.95							
T_xSS-10	0.65	106	0.679	0.512	4	0.94							

Table 2. T_xSS and DSS tests performed on the reconstituted Champlain silt.

Test No	γ_{cyc} (%)	σ'_c (kPa)	e_i	e_c	OCR	B	Test No	γ_{cyc} (%)	σ'_c (kPa)	e_i	e_c	OCR	B
T_xSS-1	0.58	101	0.613	0.548	1.0	0.96	DSS-1	0.12	103	0.681	0.547	1	-
T_xSS-2	0.28	75	0.675	0.610	1.0	0.97	DSS-2	0.15	103	0.621	0.540	1	-
T_xSS-3	0.74	96	0.641	0.550	2.0	1.00	DSS-3	0.21	105.0	0.651	0.533	2	-
T_xSS-4	0.44	89	0.750	0.528	2.0	0.97	DSS-4	0.26	109.0	0.614	0.532	2	-
T_xSS-5	0.91	100	0.668	0.501	4.0	0.95	DSS-5	0.43	93.0	0.651	0.486	4	-
T_xSS-6	0.55	102	0.643	0.485	4.0	0.95	DSS-6	0.27	102.0	0.626	0.500	4	-

The area delimited by the loops decreases from cycle to cycle and represents the energy dissipated in the material. As T_xSS cyclic tests are performed in strain control conditions, a relationship must be established between the cyclic shear stress and the cyclic shear strain to use the strain-control test results in the existing liquefaction charts which are based on the cyclic shear resistance ratio, CRR. In this study, a relationship between cyclic shear strain, cyclic shear stress, and pore pressure are established through the energy concept [17]. The normalized unit energy, W_s is defined as the energy dissipated per unit volume of soil divided by the initial effective confining pressure. In a cyclic test, the dissipated energy per unit volume can be determined by integrating area bound by stress-strain hysteresis loops as calculated in Eq. (3) [18].

$$W_s^{0.5} = \left[\frac{1}{2\sigma'_{v0}} \sum_{i=1}^{n-1} (\tau_i + \tau_{i+1})(\gamma_i - \gamma_{i+1}) \right]^{0.5} \quad (3)$$

Where $W_s^{0.5}$ is the dissipated energy; τ and γ are the calculated cyclic shear stress and cyclic shear strain at the incrementation of loading i and $i + 1$. Figure 4(a) shows the relationship between the pore pressure ratio, R_u and the dissipated energy, $W_s^{0.5}$ for the L-TM2 silt samples. To obtain this function, values of $W_s^{0.5}$ to each T_xSS test is normalized by a constant (a) which is represented in Fig. 4(b). It is important to notice that this constant depends on OCR, density and shear strain amplitude. Its decrease reflects the ability of a material to generate pore pressure. The samples with higher values of over-consolidation ratio or with a higher density may show higher values for the constant (a) as presented in Fig. 4(b).

The first hysteresis loop can also be used in the estimation of the small-strain shear stiffness (G_{max}). In addition, G_{max} and G/G_{max} can be evaluated with T_xSS tests performed from very low to high shear strains. But in this study, the G_{max} is evaluated from measurements of shear wave velocity and the degradation curve, G/G_{max} is evaluated indirectly after calibration of theoretical model on the first hysteresis loops. In fact, to determine the cyclic resistance ratio (CRR), the small-strain shear stiffness (G_{max}) and the first hysteresis loop should be used to calibrate numerical model behavior that should satisfactorily replicate the cyclic shear response of the experimental tests. The unique function between the dissipated energy and the pore pressure is used with the numerical model behavior to perform an effective stress analysis using FLAC7 [19].

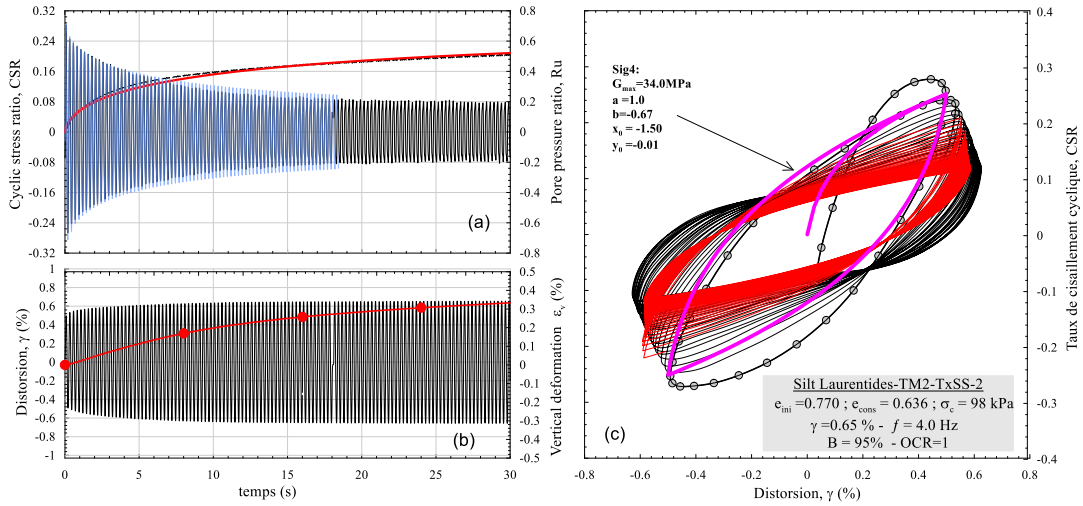


Figure 3. T_xSS tests (experimental and computed) results for a reconstituted L-TM2 silt sample

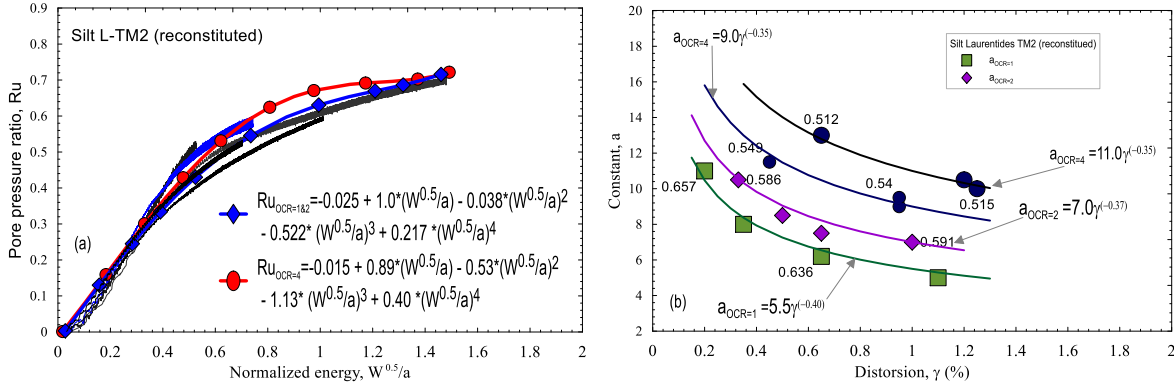


Figure 4. Pore water pressure ratio as a function of the normalized energy and Constant (a) as a function of shear strain for L-TM2 silt samples (a, b).

This approach makes it possible to consider the effect of the pore pressure and the soil degradation on the cyclic resistance. This is an advantage of this approach compared to most existing methods that assume the CSR and the G/G_{max} were not affected by the build of pore pressure [10]. In this approach, the sig4 degradation function is used to calibrate a theoretical model on the first experimental hysteresis loop. A sig4 function is given by the equation [4].

$$\frac{G}{G_{max}} = y_0 + \frac{a_1}{1 + e^{\frac{(-\log_{10}(\gamma) - x_0)}{b_1}}} \quad (4)$$

Where a_1 , b_1 , x_0 and y_0 are parameters characterizing the sig4 degradation model and γ is the shear strain in percentage. Figure 4(c) shows the calibrated sig4 model used for a T_xSS test. The values of the parameters for the calibration model are: $G_{max}=34.0MPa$, $a_1=1.0$, $b_1=-0.67$, $x_0=-1.50$ and $y_0=0.006$. The shear strength reduction and the decrease in the soil stiffness during the increasing of the pore pressure are considered by using the equation (5):

$$G_i = G_{i-1} (1 - Ru)^\alpha \quad (5)$$

The α is a constant that depends on the soil material, the soil density and the OCR. For the granular material this constant worth generally 0.5 [20], but this constant can vary between 0.5 to 2.5 for the silty soils.

Analysis of results

In this study, the number of cycles required to cause cyclic failure (or liquefaction), N_c is defined as the number of cycles to reach an excess pore water pressure ratio, R_u of 0.7. This value is determined by applying the cyclic stress τ_{cyc} in the numerical modeling of the soil samples in FLAC. Results obtained from numerical simulation of cyclic stress control tests are plotted in Figs. 5. The Fig. 5(a) Shows the values of the computed cyclic resistance ratio (CRR) versus the number of cycles to liquefy, N_c ($R_u=0.7$) at different OCRs (1, 2 and 4), densities for an initial confining pressure of about 100 kPa. The Fig.5(a) shows an increase of the cyclic resistance ratio with the over consolidation ratio (OCR). The effect of the OCR has already established

by previous studies (e.g., [5], [21]). The Fig. 5(a) shows also a decrease in the cyclic resistance ratio with the increase of the number of cycles of the apply cyclic stress, τ_{cyc} . This result is normal for any type of soil which exhibits a decrease of its resistance with the duration of the cyclic shear stress. It is possible to notice that the L-TM2 sandy silt has shown at lower density a higher cyclic resistance than the L-TM2 silt. Higher values of shear wave velocity were also obtained for the sandy silt (Fig. 2(b)). These results can be due to the soil fabric effect because soils are more resistant to liquefaction in intact conditions ([22] , [23]) To replicate the field conditions, it is not enough to reconstitute samples at the same in situ density, OCR and confining effective stress, it is preferable to consider the same normalized shear velocity with the previous parameters. However, the comparison between these silty soils may not be completed because their particles size distributions are different.

Figure 5(a) shows a comparison between the compute cyclic resistance ratio for the L-TM2 silts and direct measurements of cyclic resistance ratio obtained from DSS tests of previous studies in literature on the Frazer River silt [21] and on the Gracefield silt [24]. All the samples are normally consolidated. The results obtained in this study are consistent with other results. The Fig. 5b) shows that the comparison between the computed cyclic resistance and the direct calculated cyclic resistance with the number of cycles of loading obtained from Direct simple shear tests performed at different OCR (1, 2, and 4) for the Champlain silt. The DSS tests had been performed in stress control and the rupture criterion was considered when the samples deformation reaches a threshold value of 3.0% in single amplitude as proposed by other studies [5]. We can see that at each OCR (1, 2 and 4) value and at each comparable density values the two approaches show consistent results.

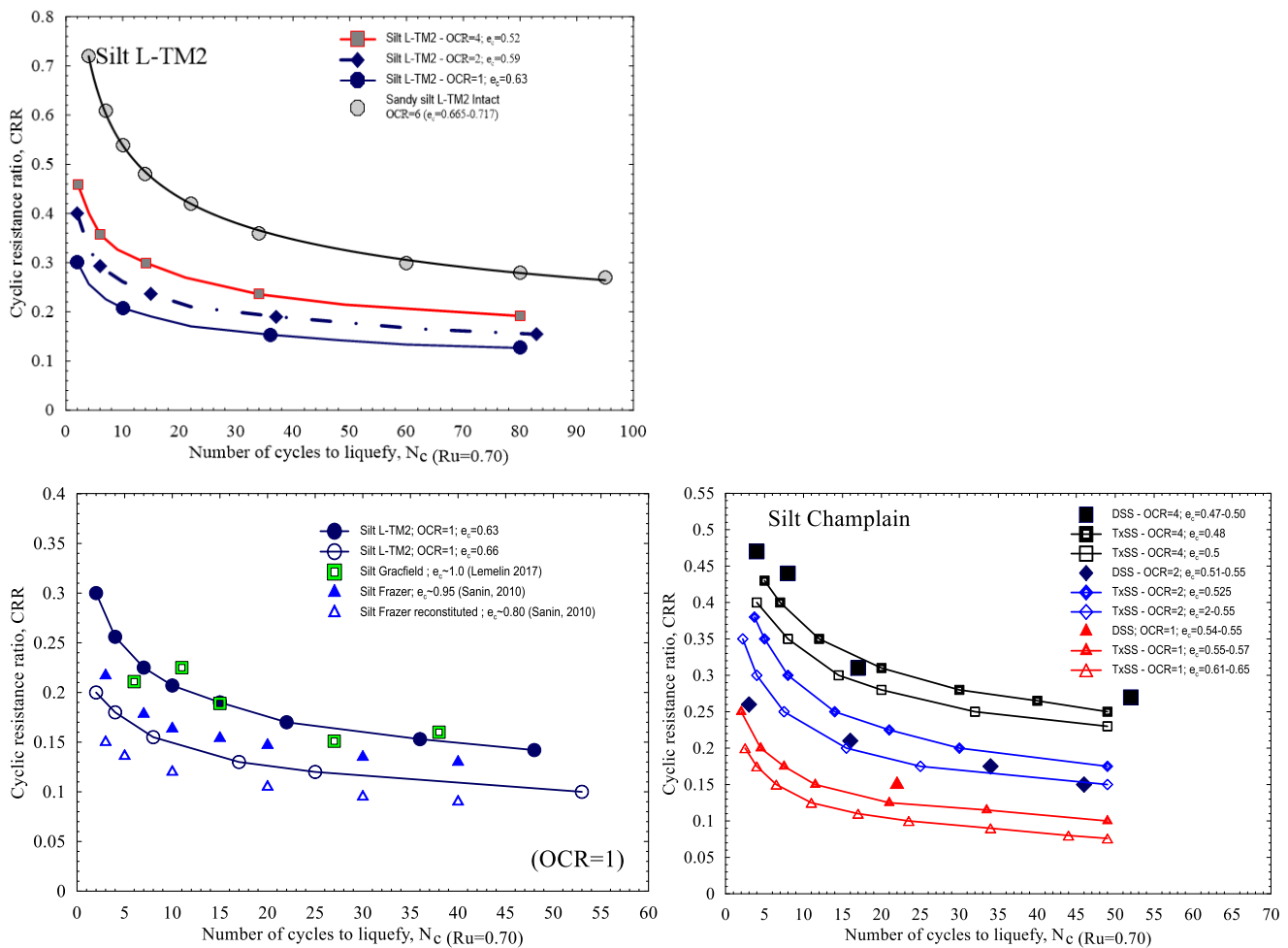


Figure 5. (a) Computed CRR- N_c ($R_u=0.7$) for the reconstituted L-TM2 silt at different OCRs (1, 2 and 4) and for the intact Sandy silt L-TM2 (b) comparison between computed cyclic resistance ratio (CRR) of the reconstituted L-TM2 silt and cyclic resistance obtained from previous study in literature on silty soils (c) comparison between Computed CRR- N_c ($R_u=0.7$) and direct CRR- N_c ($\gamma=3\%$) values obtained from DSS tests for the reconstituted Champlain silt at different OCRs (1, 2 and 4).

The Shear wave velocity is one of the parameters used in engineering practice to establish liquefaction chart. In this study, it is also used to build liquefaction charts to make the comparison possible with existing liquefaction charts. In Fig. 6, the computed cyclic resistance ratio (CRR) obtained from the combined approach based on TxSS tests and numerical simulation and from the direct cyclic resistance ratio obtained from DSS tests are plotted against the normalized shear wave velocity, V_{s1} .

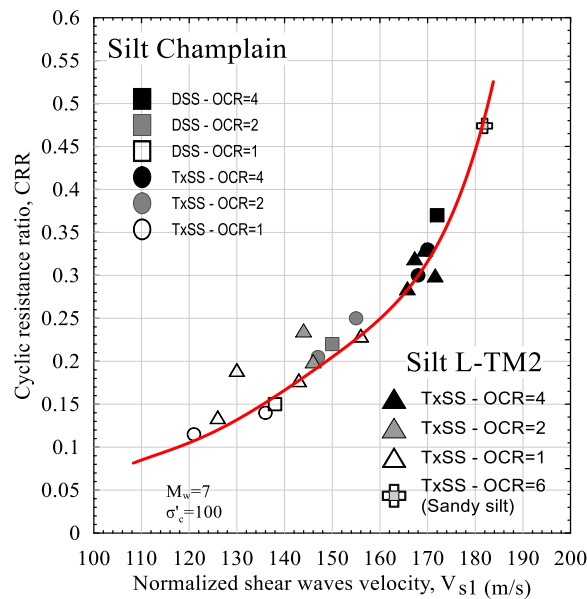


Figure 6. Computed CRR- V_{s1} curves of TxSS tests on Laurentides TM2 and Champlain silts for an earthquake magnitude, M_w of 7.5 and for an initial confining pressure of 100 kPa.

The CRR values are evaluated for the reconstituted Champlain and L-TM2 silt samples at different OCR (1, 2, and 4) and for L-TM2 sandy silt for an earthquake magnitude, M of 7.5, and for an initial confining pressure of 100 kPa. The figure 6 shows also for the silty soils studies a good tender line given the relationship between the liquefaction resistance and the normalized shear wave velocity. This figure indicates that the computed cyclic resistance ratio increases with the increase in the soil's OCR and its normalized shear velocity. The bottom of the chart is represented by normally consolidated silty samples with a normalized shear velocity below 145 m/s and with a cyclic resistance (CRR) to the liquefaction less than 0.17. The middle of the chart is represented by overconsolidated silty samples at OCR=2 with V_{s1} values below 160 m/s and with a CRR less than 0.25. The upper part of the chart is represented by samples with higher OCR and CRR values. Previous studies had been already mentioned that the lower end of liquefaction charts corresponds to normally consolidated sites that are susceptible to flow liquefaction and the upper corresponds to overconsolidated sites that are susceptible to cyclic mobility [25]. However, no flow liquefaction was observed for all tested silty samples in this study. The rupture described as liquefaction corresponds to the cyclic softening which is called cyclic mobility in granular soils. In addition, it should be noted that the density, the preshaking, the age as the overconsolidation can influence the position of a soil sample on the liquefaction chart [26].

Figure 6 shows also consistent results between DSS tests performed on the Champlain silt and the combined TxSS tests and numerical simulations performed all tested silts. The results show that the TxSS apparatus gives excellent experimental data that can be used to establish reliable soil behavior models. They also that the shear wave velocity is a good parameter that can be used as a reference to reconstitute sample and to assess soils liquefaction.

CONCLUSIONS

In this study, a new method based on laboratory tests and numerical simulations is used to assess the liquefaction potential of three silty soils. The laboratory tests included measurement of shear wave velocity through P-RAT system and cyclic resistance by the TxSS apparatus. The numerical simulations are performed with calibrated theoretical models on the experimental results considering the relationships between the generated pore pressure and the dissipated energy and the soil degradation during the cyclic tests. This is an important advantage of this approach which does not neglect the effect of the pore pressure and the cyclic degradation on the soil liquefaction resistance.

To validate this approach, direct simple shear tests are performed on the Champlain silt at different OCRs (1,2 and 4) and at different density values. The combined approach shows consistent cyclic resistance to liquefaction with the direct simple shear tests. The results are also consistent with previous studies on silty soils. The consistent results show that the TxSS apparatus can be used to obtain excellent experimental test data to establish reliable soil behavior models. In addition, they show that the shear wave velocity is an excellent parameter to use as a reference to reconstitute sample at the same in situ characteristic and to assess soils liquefaction. And finally, this study shows that the new combined approach is promising for the assessment of liquefaction of fine-grained soils.

ACKNOWLEDGMENTS

Acknowledge to the Sherbrooke University and to Hydro Québec.

REFERENCES

- [1] Seed H, Idriss I. Simplified procedure for evaluating soil liquefaction potential 1971;97:1249–73.
- [2] Boulanger RW, I.M. Idriss. CPT And SPT Based Liquefaction Triggering Procedures. Center for Geotechnical Modeling / Department of Civil and Environmental Engineering University of California Davis, California; 2014.
- [3] Robertson PK. Comparing CPT and Vs Liquefaction Triggering Methods. *J Geotech Geoenvironmental Eng* 2015;141:04015037 (10 pp.). doi:10.1061/(ASCE)GT.1943-5606.0001338.
- [4] Boulanger RW, Idriss IM. Liquefaction susceptibility criteria for silts and clays. *J Geotech Geoenvironmental Eng* 2006;132:1413–26. doi:10.1061/(ASCE)1090-0241(2006)132:11(1413).
- [5] Donahue JL. The liquefaction susceptibility, resistance, and response of silty and clayey soils. University of California, Berkeley, 2007.
- [6] Boulanger RW, Meyers MW, Mejia LH, Idriss IM. Behavior of a fine-grained soil during the Loma Prieta earthquake. *Can Geotech J* 1998;35:146–58.
- [7] Sunitsakul J. Dynamic Behavior of Silty Soils. Thesis. Oregon State University, 2004.
- [8] Karray M, Hussien MN, Jeudy B, Cheriked M, Grenier S. Use of Shear wave velocity to assess liquefaction potential of silty soils at the new Champlain Bridge, Ottawa: 2017.
- [9] Kuerbis R, Vaid YP. Sand sample preparation - the slurry deposition method. *Soils Found* 1988;28:107–18.
- [10] Poncelet N. Élaboration et implémentation d'un protocole de laboratoire pour l'étude du potentiel de liquéfaction de résidus miniers. Mémoire de maîtrise. Université De Montréal, 2012.
- [11] Karray M, Romdhan MB, Hussien MN, Ethier Y. Measuring shear wave velocity of granular material using the piezoelectric ring-actuator technique (P-RAT). *Can Geotech J* 2015;52:1302–17. doi:10.1139/cgj-2014-0306.
- [12] Karray M, Lefebvre G, Ethier Y, Bigras A. Influence of particle size on the correlation between shear wave velocity and cone tip resistance. *Can Geotech J* 2011;48:599–615. doi:10.1139/t10-092.
- [13] Hardin BO, Drnevich VP. Shear Modulus And Damping In Soils: Measurement And Parameter Effects. *Am Soc Civ Eng J Soil Mech Found Div* 1972;98:603–24.
- [14] Biu MT. Influence of some particle characteristics on the small strain response of granular materials. Thesis. University Of Southampton, 2009.
- [15] Choo H, Burns SE. Shear wave velocity of granular mixtures of silica particles as a function of finer fraction, size ratios and void ratios. *Granul Matter* 2015;17:567–78. doi:10.1007/s10035-015-0580-2.
- [16] Cheriked M, Lemire R, Karray M, Mahmoud NH. Experiment Setup for simple shear tests in a triaxial cell, Québec: 2015.
- [17] Berrill JB, Davis RO. Energy Dissipation And Seismic Liquefaction Of Sands: Revised Model. *Soils Found* 1985;25:106–18.
- [18] Green RA, Mitchell JK, Polito CP. An Energy-Based Excess Pore Pressure Generation Model for Cohesionless Soils. *Proc. John Booker Meml. Symp. Syd., Sydney, New South Wales, Australia: 2000.*
- [19] Itasca. FLAC - Fast Lagrangian Analysis of Continua, Version 6. Itasca Consulting Group, Inc; 2007.
- [20] Matasovic N, Vucetic M. Cyclic Characterization of Liquefiable Sands. vol. 119. 1993. doi:10.1061/(ASCE)0733-9410(1993)119:11(1805).
- [21] Sanin M. Cyclic shear loading response of Fraser River delta silt. Thesis. University of British Columbia, 2010.
- [22] Wijewickreme D, Sanin MV. Cyclic shear response of undisturbed and reconstituted low-plastic Fraser River silt. *Geotech. Earthq. Eng. Soil Dyn. IV Congr. 2008 - Geotech. Earthq. Eng. Soil Dyn. May 18 2008 - May 22 2008, ASCE - American Society of Civil Engineers; 2008.* doi:10.1061/40975(318)88.
- [23] Hoeg K, Dyvik R, Sandbaekken G. Strength of undisturbed versus reconstituted silt and silty sand specimens. *J Geotech Geoenvironmental Eng* 2000;126:606–17. doi:10.1061/(ASCE)1090-0241(2000)126:7(606).
- [24] Lemelin ean-C. Étude du comportement statique et cyclique d'un dépôt de sols à grains fins de Gracefield (Québec). Mémoire de maîtrise. LAVAL, 2017.
- [25] Mital U, Mohammadnejad T, Andrade JE. Flow liquefaction instability as a mechanism for lower end of liquefaction charts. *J Geotech Geoenvironmental Eng* 2017;143:04017065 (9 pp.). doi:10.1061/(ASCE)GT.1943-5606.0001752.
- [26] Dobry R, Abdoun T. An Investigation Into Why Liquefaction Charts Work: A Necessary Step Toward Integrating The States Of Art And Practice, Santiago, Chile: 2011, p. 13–45.